

An Online Structurally Constrained LQR Design for Damping Oscillations in Power System Networks

Abhishek Jain¹, Aranya Chakraborty¹ and Emrah Biyik²

Abstract—This paper presents an online distributed control design for suppressing inter-area oscillations in large power systems under structural constraints posed on the underlying communication network. The presence of multiple clusters of generators in a power system results in several inter-area oscillation modes. By modal analysis, we first show that the contribution of each inter-area mode on the electromechanical state response of the generators is heavily dependent on the perturbed initial state of the system. We then take advantage of this observation to design structural constraints on the communication graph. A parallelized constrained linear quadratic regulator (LQR) design is then proposed to balance the trade-off between performance and the level of sparsity induced in the network. Algorithms for practical implementation of the design are provided. Results are compared with the full order LQR, and illustrated on the New England 39-bus power system model.

Index Terms—Distributed control, constrained control, power systems, modal analysis.

I. INTRODUCTION

Inter-area oscillations are a growing concern for the rapidly modernizing power transmission networks. These lightly damped oscillations occur in the frequency range of 0.1-2 Hz (called inter-area modes), and if not well-damped then they can cause undesirably large swings in power flows across long-distance tie-lines [1]. Traditional controllers such as power system stabilizers (PSS) are designed to damp only local oscillations (above 2 Hz), and are often not very effective in damping these lower-frequency modes [2]. To address this problem, wide-area controllers such as wide-area PSS and Flexible AC Transmission System (FACTS) devices have been proposed in the literature, using system-wide output feedback instead of local feedback. These controllers aim to increase the controllability of inter-area modes using different tools of modern control theory such as robust and optimal control [3], [4]. A tutorial on these different methods has recently been reported in [5].

However, one drawback of the above-mentioned wide-area control methods is that they result in a centralized control architecture, which necessitates continuous transmission and reception of signals from a central control entity. For example, a vast majority of wide-area control has been proposed to be LQR-type designs, where the PSS of every generator must communicate with that of every other generator in real-time

for actuating the control. Quite naturally, these designs are not very scalable as they require an extremely dense communication graph with tens of thousands of communication links transferring massive volumes of feedback data. Centralized execution is also not very resilient to extraneous failures and attacks. Therefore, in recent years power system operators are gradually moving away from centralized control, and inclining more towards *distributed* control, where the communication graph is sparse. Some of the few works that have taken this approach for wide-area control are [6], [7]. The work in [6] uses a sparsity-promoting optimal control strategy to first determine the control feedback structure, and then optimize the \mathcal{H}_2 -norm of the system, whereas [7] uses geometric measures for selection of control loops so as to maximize the controllability and observability of the inter-area modes. These designs, however, assume the precise location of the disturbance entering the grid dynamics to be exactly known, which in practice can be a rather limiting assumption.

In contrast, in this paper we propose a sparse LQR design where the sparsity pattern is decided online after a disturbance happens in the grid, based on the residues of the excited modes reflected in the predicted outputs. Note that many papers such as [7] have designed controllers based on modal participation factors that are only based on the natural dynamics of the power system. Our approach is slightly different from them as residues not only depend on the system poles but also on the input and output matrices of the state-variable model. Hence, depending on where the disturbance enters, the residues of the characteristic modes on the same outputs can be different from one event to another. Thus, the sparsification and the resulting overall structure of the communication network in our design are directly influenced by the physical characteristics of the grid. This is an important feature that separates our design from state-of-the-art control of other cyber-physical systems, where the cyber and the physical infrastructures are often designed independent of each other.

Our objective is to design a state-feedback distributed controller, which is both stabilizing and requires less number of communication links. Hence, we solve a structurally constrained infinite-horizon LQR problem. Since it is assumed that the location and strength of the exogenous disturbance is unknown, we first use the post-disturbance system state to determine the sets of generators participating most in the excited modes. Using this information, we build our communication graph for distributed control, and obtain the structure of the feedback matrix to be used as a constraint in

¹Abhishek Jain and Aranya Chakraborty are with the Department of Electrical Engineering, North Carolina State University, Raleigh, NC, USA ajain18@ncsu.edu, aranya.chakrabortty@ncsu.edu

²Emrah Biyik is with the Department of Energy Systems Engineering, Yasar University, Izmir, Turkey emrah.biyik@yasar.edu.tr

the LQR problem. This problem is solved using an iterative algorithm which assures closed-loop stability of the system. A parallel implementation strategy for computing multiple versions of the controller, depending on different levels of sparsity, is proposed. Analyzing the trade-offs between control performance and the level of sparsity induced, the most effective controller is chosen. Results are validated using simulations on a 39-bus New England power system model. Simulations show that the designed controller is effective in promoting sparsity as well as introducing considerable damping into the system.

II. PROBLEM FORMULATION

A. System Model & Control Objective

We consider an arbitrarily connected power system network with n generators. A third-order classical model of synchronous generators is used to represent their swing and excitation dynamics, with state variables δ_i, ω_i, E_i that represent the generator phase angle, rotor velocity and quadrature-axis internal EMF, respectively [1]. The control input to the generator is chosen as the excitation field voltage E_{F_i} . Let m be the total number of system states, $x_i(k) = [\Delta\delta_i(k), \Delta\omega_i(k), \Delta E_i(k)]'$ be the linearized i^{th} generator state vector, and $u_i(k) = \Delta E_{F_i}(k)$ be the i^{th} scalar control input at the time-step k . All three states are assumed to be measurable from PMUs located at every generator bus. We model the linearized power system model, discretized with a sampling time of T_s , as:

$$x(k+1) = Ax(k) + Bu(k) + \tilde{B}d(k), \quad (1a)$$

$$u(k) = Kx(k), \text{ and } x_0 \triangleq x(0), \quad (1b)$$

where $x(k)=[x_1(k)', \dots, x_n(k)']'$, $u(k)=[u_1(k), \dots, u_n(k)]'$, $A \in \mathbb{R}^{m \times m}$ is the system matrix, $B \in \mathbb{R}^{m \times n}$ is the control input matrix, $\tilde{B} \in \mathbb{R}^{m \times n}$ is the disturbance input matrix, and $d(k)$ is the scalar impulsive disturbance at $k=0$. The quantity $\tilde{B}d(k)$ is assumed to be unknown for control design assuming that the location and severity of the fault is not known *a priori*. The matrix $K \in \mathbb{R}^{n \times m}$ is the linear feedback gain for supplementary control (i.e. on top of the existing PSS control). It is assumed that the pair (A, B) is stabilizable.

Our control objective is to design a distributed and sparse state-feedback controller $u(k)$ to damp the closed-loop oscillations of the model (1). We pose the problem as minimizing the infinite-horizon LQR cost function:

$$J_\infty(x_0) = \sum_{k=0}^{\infty} \{x(k)'Qx(k) + u(k)'Ru(k)\}, \quad (2)$$

under a structural constraint $K \in \Omega$, where $\Omega \in \mathbb{R}^{n \times m}$ is a set of matrices with pre-specified zero locations. $Q > \mathbf{0}$, $R > \mathbf{0}$ are the state and control weighting matrices respectively, where Q is designed such that the square of the differences of the generator angles (proportional to the power transfer between generators), along with the quadratic energy of the rest of

the states are penalized. This translates to the state-weighting term in (2) as:

$$x(k)'Qx(k) = \sum_{i=1}^n \sum_{j>i}^n (\Delta\delta_i(k) - \Delta\delta_j(k))^2 + \sum_{i=1}^n \tilde{x}(k)' \tilde{x}(k), \quad (3)$$

where \tilde{x} is the vector of all linearized states except the rotor angle $\Delta\delta$. Let the notation I_z denote an identity matrix of size z , and let the matrix of all ones be denoted by $\mathbb{1}_{ab} \in \mathbb{R}^{a \times b}$. To obtain the form in (3), the state-weighting matrix Q is constructed with the transformation [8]: $Q \triangleq \mathcal{T}'\tilde{Q}\mathcal{T}$, where $\tilde{Q} = \begin{pmatrix} \mathcal{L} & \\ & I_{m-n} \end{pmatrix}$ is a block diagonal matrix, $\mathcal{L} = nI_n - \mathbb{1}_{n1}\mathbb{1}'_{n1}$ is the matrix for difference in angles, and the transformation matrix \mathcal{T} is as given in [8].

B. Distributed Control

The feedback gain matrix K in (1b) can be designed by a central control authority, which then communicates its individual rows $K(i, :)$, $\forall i=1, \dots, n$, to the corresponding generator actuators, i.e. $u_i(k) = K(i, :)x(k)$, $\forall i=1, \dots, n$. Then, depending on the non-zero entries of $K(i, :)$, the i^{th} controller can communicate and receive the corresponding states from other generators to calculate its own actuator control input. Thus, a sparse K will result in a sparse communication graph, thereby enabling the control to be implemented in a distributed way. The following section provides modal analysis of the system, which forms a basis for constructing the sparse structure of K .

III. MODAL ANALYSIS

& STRUCTURE OF STATE FEEDBACK MATRIX

A. Modal Participation

Once a disturbance is detected, every generator must send their initial state information $x_i(0)$ to a central authority such as the Independent System Operator (ISO), which then forms the vector x_0 . The ISO will then estimate the modal residues of $x(k)$ from which it can decide the sparsity structure of the wide-area communication network. From linear system theory it follows that $x(k)=A^k x_0$ for the unforced open-loop system. Equivalently, one may also write the state response in the modal decomposition form as:

$$x(k) = \bar{\mathcal{M}}(\lambda_1^k, \dots, \lambda_m^k)', \quad (4)$$

where $\{\lambda_j\}$ are the eigenvalues of A (assumed to be distinct); $\bar{\mathcal{M}} = \text{col}(\alpha_1\rho_1, \dots, \alpha_m\rho_m)$ where $\text{col}(\cdot)$ denotes a matrix of column vectors; $\{\rho_i\}$ are the right eigenvectors of A ; and $\{\alpha_i\}$ are constant scalars. Denoting $\mathcal{M} = \text{col}(\rho_1, \dots, \rho_m)$ as the modal matrix, $\Lambda = \text{diag}(\lambda_1, \dots, \lambda_m)$, and $\alpha = (\alpha_1, \dots, \alpha_m)'$, from (4) we get: $x(k) = \mathcal{M}\Lambda^k\alpha$. Comparing this equation with the state equation in the initial value form, and using the identity $A^k = \mathcal{M}\Lambda^k\mathcal{M}^{-1}$, we get:

$$\alpha = \mathcal{M}^{-1}x_0. \quad (5)$$

The individual states can also be written in their modal form as $x_i(k) = \sum_{j=1}^m \bar{\rho}_{ij}\lambda_j^k$, where each $\bar{\rho}_{ij}=\alpha_i\rho_j$. This shows that once the ISO knows x_0 (which depends on the unknown exogenous disturbance), it can estimate α , and therefore, the

modal coefficients (residues) $\bar{\rho}_{ij}$. Since the high-frequency modes of the electromechanical states are assumed to be sufficiently damped with installed PSSs as primary controllers, our design will be focused only on the inter-area oscillation modes, i.e., the first $n-1$ modes in increasing order of their frequency. However, we will define dominance of these modes not based on their frequencies, but on their output residues. For example, consider a power system with five generators (i.e. $n = 5$), with each generator considered as a coherent area in itself, yielding $n-1 = 4$ inter-area modes. Next, approximating the electromechanical state response by neglecting the participation of high-frequency modes, we get:

$$\begin{aligned} S_1 : x_1(k) &\approx \bar{\rho}_{11}\lambda_1^k + \bar{\rho}_{12}\lambda_2^k + \bar{\rho}_{13}\lambda_3^k + \bar{\rho}_{14}\lambda_4^k + b_1(k), \\ S_2 : x_2(k) &\approx \bar{\rho}_{21}\lambda_1^k + \bar{\rho}_{22}\lambda_2^k + \bar{\rho}_{23}\lambda_3^k + \bar{\rho}_{24}\lambda_4^k + b_2(k), \\ S_3 : x_3(k) &\approx \bar{\rho}_{31}\lambda_1^k + \bar{\rho}_{32}\lambda_2^k + \bar{\rho}_{33}\lambda_3^k + \bar{\rho}_{34}\lambda_4^k + b_3(k), \\ S_4 : x_4(k) &\approx \bar{\rho}_{41}\lambda_1^k + \bar{\rho}_{42}\lambda_2^k + \bar{\rho}_{43}\lambda_3^k + \bar{\rho}_{44}\lambda_4^k + b_4(k), \\ S_5 : x_5(k) &\approx \bar{\rho}_{51}\lambda_1^k + \bar{\rho}_{52}\lambda_2^k + \bar{\rho}_{53}\lambda_3^k + \bar{\rho}_{54}\lambda_4^k + b_5(k), \end{aligned} \quad (6)$$

where $b_i(k) = x_i^{dc} + \sum_{j=1}^4 \bar{\rho}_{ij}^* \lambda_j^{*k}$, x_i^{dc} represents the DC mode of the i^{th} state, and $(*)$ denotes complex conjugation since $\{\bar{\rho}_{ij}\}$ and $\{\lambda_j\}$ are, in general, complex numbers. We assume the residues $\bar{\rho}_{11}$, $\bar{\rho}_{22}$, $\bar{\rho}_{31}$, $\bar{\rho}_{41}$, $\bar{\rho}_{52}$, marked in boldface, to be dominant residues. Dominance is defined such that all $|\bar{\rho}_{ij}| \geq \mu$, where μ is a pre-specified threshold, the choice of which is further explained in Section IV-C and Algorithm 1.

In other words, we assume that only the inter-area modes λ_1, λ_2 are substantially excited by the incoming disturbance while the other inter-area modes have much poorer participation in the states. The residue magnitudes are then collected in a so-called modal participation (MP) matrix that shows which generators contribute most to the excitation of which dominant mode. For this example, generators S_1, S_3, S_4 contribute significantly to mode λ_1 , and generators S_2, S_5 to mode λ_2 . Information about this grouping is used to decide the topology of communication. Detailed description of this will be given in the next subsection. Note that two different disturbance events can result in two significantly different x_0 , and hence, two significantly different MP matrices, indicating different sets of generators influencing different combinations of the inter-area modes. It is important for a controller to be aware of this dominance property instead of an offline controller that is agnostic to it. This is why our controller is designed in real-time after the fault happens.

B. Proposed Communication Strategy

For the 5-machine example in (6), the following control strategy is proposed:

- 1) For suppressing the amplitude of oscillations excited by mode λ_1 , since the residues $\bar{\rho}_{11}, \bar{\rho}_{31}, \bar{\rho}_{41}$ are dominant, S_1, S_3, S_4 communicate.
- 2) For suppressing the amplitude of oscillations excited by mode λ_2 , since the residues $\bar{\rho}_{22}, \bar{\rho}_{52}$ are dominant, S_2, S_5 communicate.

Similar to [9], we also make the assumption that the controller only changes the damping of the closed-loop inter-area modes, and does not change the frequency of these modes significantly. Steps to construct the feedback structure are given in the following.

C. Construction of Feedback Structure

Following the strategy proposed in the previous section, for the control $u = Kx$, the state feedback matrix structure for the 5-machine example in (6) is thus constructed as:

$$\begin{pmatrix} u_1 \\ u_2 \\ u_3 \\ u_4 \\ u_5 \end{pmatrix} = \underbrace{\begin{bmatrix} \times & 0 & \times & \times & 0 \\ 0 & \times & 0 & 0 & \times \\ \times & 0 & \times & \times & 0 \\ \times & 0 & \times & \times & 0 \\ 0 & \times & 0 & 0 & \times \end{bmatrix}}_{\Omega} \begin{pmatrix} x_1 \\ x_2 \\ x_3 \\ x_4 \\ x_5 \end{pmatrix}, \quad (7)$$

where (\times) indicates an arbitrary scalar value, and Ω is the set of matrices with the specific structure with $K \in \Omega$. The procedure for constructing Ω is then generalized as follows.

Let $\lambda_1, \dots, \lambda_{n-1}$ be the modes of interest which we wish to suppress via a sparse state-feedback control $K \in \Omega$. Let \mathcal{R} be the $n(n-1)$ -tuple of all modal coefficients, i.e. $|\bar{\rho}_{ij}| \in \mathcal{R}, \forall i = 1, \dots, n$, and $\forall j = 1, \dots, n-1$. Then, for each $\lambda_j, j \in \{1, \dots, n-1\}$, we obtain the set of indices:

$$\Xi_j \triangleq \{i \in (1, \dots, n) \mid |\bar{\rho}_{ij}| \geq \mu, \forall |\bar{\rho}_{ij}| \in \mathcal{R}\}, \quad (8)$$

where $\mu \in \mathbb{R}$ is some threshold for dominant coefficient selection (chosen as the arithmetic mean of $\text{vec}(\bar{\mathcal{M}})$, and iterated via parallelization as described in Section IV-C). Let $r_j \triangleq \text{card}(\Xi_j)$, where $\text{card}(\cdot)$ denotes the number of elements of the specified set (cardinality). Construction of the feedback matrix structure is then given by:

$$\Omega(i, j) = \begin{cases} \times, & \text{if } (i, j) \in \bigcup_{j=1}^{n-1} Z_j \\ 0, & \text{otherwise,} \end{cases} \quad (9)$$

where Z_j is the set of r_j^2 2-tuples over Ξ_j . For the example considered above in (6),(7), the sets/tuples \mathcal{R}, Ξ_j, Z_j , for the mode λ_1 , are given as:

$$\begin{aligned} \mathcal{R} &= (|\bar{\rho}_{11}|, |\bar{\rho}_{12}|, \dots, |\bar{\rho}_{53}|, |\bar{\rho}_{54}|), \text{ with } \mathcal{R} \text{ a 20-tuple,} \\ \Xi_1 &= \{1, 3, 4\}, \text{ with } r_1 = 3, \\ Z_1 &= \{(1, 1), (1, 3), (1, 4), (3, 1), (3, 3), (3, 4), (4, 1), \dots \\ &\quad \dots (4, 3), (4, 4)\}, \text{ with } \text{card}(Z_1) = 9. \end{aligned}$$

The sets Ξ_2, Z_2 can be determined similarly, and the structure of Ω in (7) can then be formed using (9) (sets Ξ_3 and Ξ_4 will be empty). Next, we formulate our control design procedure using LQR, with the state-feedback structure constructed above as a constraint.

IV. CONSTRAINED LQR CONTROL

A constrained LQR formulation for the power system is done by specifying structural constraints on the feedback matrix, and then using a generalized discrete algebraic Riccati equation (GDARE) method to obtain a stabilizing constrained K .

A. Discrete Linear Quadratic Regulator

Recall from (2) that the infinite-horizon quadratic cost to be minimized is:

$$J_\infty(x_0) = \sum_{k=0}^{\infty} \{x(k)'Qx(k) + u(k)'Ru(k)\}, \quad (10)$$

where the optimal feedback matrix K is obtained from:

$$K = -(R + B'PB)^{-1}B'PA. \quad (11)$$

The unique symmetric matrix $P > 0$ is obtained from the well-known discrete algebraic Riccati equation (DARE):

$$P = A'PA - A'PB(R + B'PB)^{-1}B'PA + Q. \quad (12)$$

In addition to the state evolution constraint (1a), we add the structural sparsity constraint $K \in \Omega$, where Ω is determined from the modal analysis procedure detailed in Section III. The constrained control problem then becomes:

$$\mathcal{P}: \quad \min J_\infty(x_0) \quad (13a)$$

$$\text{s.t. } K \in \Omega. \quad (13b)$$

Also, the solution of \mathcal{P} should provide a matrix K such that the closed-loop system matrix $A+BK$ is Hurwitz. It is clear that the nominal solution from (11) will no longer necessarily satisfy the structural constraint (13b). In the next subsection, we propose an online constrained control design method which provides a solution to the above problem.

B. Generalized Riccati Equation Method

First, we formulate the constraint (13b) in an alternative way for use in the proposed method. Let I_Ω be the indicator matrix for the structured matrix set Ω ; an example would be to replace the (\times)s with (1)s in the feedback matrix in (7). Next, let I_Ω^c be the complement of I_Ω . Then the following identity holds for the structural constraint (13b):

$$F(K) \triangleq K \circ I_\Omega^c = \mathbf{0}, \quad (14)$$

where (\circ) is the Hadamard product, and $\mathbf{0}$ is the zero matrix of appropriate dimensions. Hence the constraint $F(K) = \mathbf{0}$ is equivalent to (13b). The following theorem then assures the stability of the closed-loop system.

Theorem 1 ([10]): For the discrete-time system (1a) and control law (1b), if the state-feedback gain matrix K satisfies:

$$K + L = -(R + B'PB)^{-1}B'PA, \quad (15)$$

where L is an arbitrary matrix, and the symmetric matrix $P > 0$ is the solution of the GDARE:

$$P = A'PA - A'PB(R+B'PB)^{-1}B'PA + Q + L'(R+B'PB)L, \quad (16)$$

then the closed-loop system matrix $A+BK$ is Hurwitz. ■

The following corollary provides an appropriate choice for the matrix L so as to satisfy the structural constraint on K .

Corollary 1: To enforce the structural constraint (13b), the matrix L in Theorem 1 can be chosen as:

$$L = F(\Psi(P)), \quad (17)$$

$$\text{where: } \Psi(P) \triangleq -(R+B'PB)^{-1}B'PA. \quad (18)$$

Proof: We substitute (17)-(18) in (15) to get:

$$K = \Psi(P) - [\Psi(P) \circ I_\Omega^c] \quad (19a)$$

$$= \Psi(P) \circ [\mathbf{1}_{nm} - I_\Omega^c] \quad (19b)$$

$$= \Psi(P) \circ I_\Omega, \quad (19c)$$

where $\mathbf{1}_{nm} \in \mathbb{R}^{n \times m}$ is a matrix of all ones (since $K \in \mathbb{R}^{n \times m}$), and (19b) is the result of the distributive property (over addition) of the Hadamard product. From (19c) we see that $K \in \Omega$, and hence the particular choice of L in (17) gives the desired structure in the feedback matrix. ■

C. Algorithm for Solution of \mathcal{P}

To solve the GDARE (16) iteratively, we use the algorithm proposed in [10] but with the constraint (13b). The algorithm is also parallelized so that the problem \mathcal{P} can be solved with multiple sparsity structures, and the ones with an allowable execution time can be selected. Let p be the total number of parallelizations, i.e. we obtain $K_i \in \Omega_i, \forall i=1, \dots, p$. For each parallelization i , a threshold $\mu_i \in \mathbb{R}$ is chosen, leading to the corresponding set of dominant residues from (8). One choice to achieve this is with a ‘running mean’, i.e. taking successive arithmetic means of the residue vector $\text{vec}(\bar{M})$, so as to extract the sets of relatively large residues. These sets can then be used to construct the sparse feedback structures from (8)-(9). The above procedure is summarized in Algorithm 1, where $\bar{\mu}(\cdot)$ is the arithmetic mean function.

Algorithm 1 Running Mean Algorithm for Parallelization

- 1: Start: $\mathcal{X}_0 = \{\text{vec}(\bar{M})\}$ ▷ Set of All Coeffs.
 - 2: **for** $i \leftarrow (1, \dots, p)$ **do**
 - 3: $\mu_i = \bar{\mu}(\mathcal{X}_{i-1})$ ▷ Arithmetic Mean
 - 4: Construct $\Omega_i(\mu_i)$ from (8)-(9)
 - 5: $\mathcal{X}_i = \{|\bar{\rho}_{ij}| \in \mathcal{X}_{i-1} \mid |\bar{\rho}_{ij}| \geq \mu_i\}$ ▷ Dominant Coeffs.
 - 6: **end for**
-

From Algorithm 1, we obtain $\{\Omega_i\}_{i=1}^p$, and construct the corresponding Riccati matrices P_i , by solving the GDARE (16) with the constraint $K_i \in \Omega_i$, and then checking the local convergence of the normalized P_i iteratively (see Algorithm 2). Once the algorithm converges for a small value ϵ ($= 10^{-3}$ in our simulations), the sparse feedback matrix K_i is calculated from (15). Parallelization of the algorithm is used to obtain only those solutions which have convergence times less than a chosen threshold τ_{th} . The feedback matrices which ‘pass’ this test are then stored in the set \bar{K} .

The ‘best’ feedback matrix $K^* \in \bar{K}$ is chosen according to the following considerations, which reflect the trade-off between the level of sparsity and time-domain performance of the closed-loop system.

- 1) *Level of block-sparsity:* The number of communication links in the n -generator network is given by: $n(n+1)/2$. From (8), let $r_j \triangleq \text{card}(\Xi_j)$. Hence, the number of links corresponding to a structure Ω_i is: $g_i = \sum_{j=1}^{n-1} r_j(r_j+1)/2$. Then the level of block sparsity for the sparse graph, relative to the full graph, is defined by the sparsity index $\theta_i \triangleq 1-2g_i/n(n+1)$.

Algorithm 2 Algorithm for solution of \mathcal{P} , $\forall i = 1, \dots, p$

- 1: Obtain $P_i^{(0)}$ from (12) ▷ Initialize
 - 2: **Start:** $k = 0$, $\tau_i = 0$, $\bar{K} = \emptyset$
 - 3: $L_i^{(k+1)} = \Psi(P_i^{(k)}) \circ I_{\Omega_i}^c$ ▷ Enforce Structure Ω_i
 - 4: $P_i^{(k+1)} = A'P_i^{(k+1)}A + A'P_i^{(k+1)}B\Psi(P_i^{(k+1)}) + Q + L_i^{(k+1)'}(R+B'P_i^{(k)}B)L_i^{(k+1)}$ ▷ Solve GDARE
 - 5: **if** $\frac{\|P_i^{(k+1)} - P_i^{(k)}\|_2}{\|P_i^{(0)}\|_2} < \epsilon$ **then** ▷ Check Convergence
 - 6: $K_i = \Psi(P_i^{(k)}) - L_i^{(k+1)}$
 - 7: $\tau_i \leftarrow \tau_i^{new}$ ▷ Check Execution Time
 - 8: **if** $\tau_i < \tau_{th}$ **then**
 - 9: $\bar{K} \cup K_i \leftarrow \bar{K}$ ▷ Time-Feasible Set
 - 10: **end if**
 - 11: **else**
 - 12: $k \leftarrow k+1$ and goto step 2 ▷ Re-iterate
 - 13: **end if**
-

2) *Sub-optimal cost:* The sub-optimality index, with a $K_i \in \Omega_i$, is defined by $\xi_i \triangleq (J_{\Omega_i} - J_{opt})/J_{opt}$, where J_{Ω_i} and J_{opt} are the costs corresponding to the sparse structure Ω_i , and the unconstrained optimal control problem, respectively.

Since the full order LQR controller is optimal, forcing sparsity in the feedback structure will essentially result in sub-optimal closed-loop performance. Also, the closed-loop performance will degrade as the level of sparsity is increased. This trade-off can be analyzed by the above defined indices θ_i, ξ_i for different parallelized solutions for K_i , and is shown in Table II for our simulations.

V. SIMULATION RESULTS

We verify our design on the New England 39-bus, 10-generator power system model with a total of 130 states including the exciter, PSS, and turbine governor states. The model data is taken from the Power Systems Toolbox where some transmission line lengths and reactances are modified so that the open-loop system exhibits multiple inter-area oscillation modes, as shown in Fig. 2(a), while still representing a realistic power transmission model.

We also compare our results with the work in [6] where a similar problem is solved. The weighted sum of Frobenius norms is used for obtaining the block-sparse feedback structure, with the value of the sparsity-promoting parameter chosen as $\gamma=180$. It is noted that this design is done completely offline, and hence will give the same feedback matrix $K_{\mathcal{H}_2}$ irrespective of the location and strength of the disturbance $d(k)$ in (1). In comparison, our design is online (uses x_0), and hence the structure and values of K^* are aware of the disturbance.

The nonlinear power system model is excited via a three-phase fault on the line connecting buses 3-4, which is cleared after 0.1 secs at bus 3, and after 0.15 secs at bus 4. Once the fault is cleared, $x_0 \in \mathbb{R}^{130 \times 1}$ can be estimated from all the state measurements. As shown in Section III, x_0 contains the information regarding the residues of the dominant modes, and hence is used to construct the MP matrix (6) of the

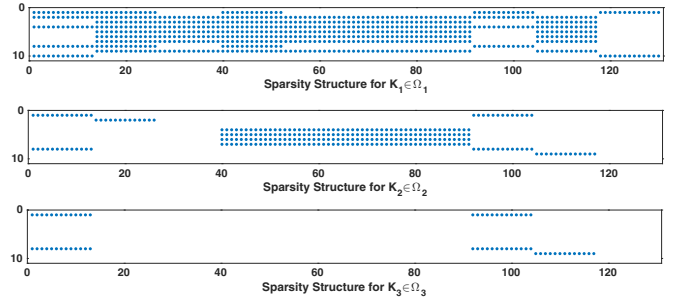


Fig. 1: Controller sparsity structures for the NE system obtained using Algorithm 1 for the three parallelized cases.

open-loop system. Next, three parallelized control designs are done for the feedback structures $\{\Omega_i\}_{i=1}^3$ obtained from Algorithm 1. Table I shows the MP matrix for the state $\Delta\omega$, with the residues in $\{\mathcal{X}_i\}_{i=1}^3$ highlighted in various colors as: (i) \mathcal{X}_1 : all colors green, orange, red; (ii) \mathcal{X}_2 : colors orange, red; and (iii) \mathcal{X}_3 : color red only. Following the approach in Section III, the sparsity patterns in the feedback controllers for the three structures are shown in Fig. 1.

Next, Algorithm 2 is implemented to obtain the block-sparse feedback matrices $\{K_i\}_{i=1}^3$, with the state-weighting matrix Q as given in (3), and the control-weighting matrix as $R = 0.1 \times I_n$. The convergence parameter is chosen as $\epsilon=10^{-3}$. Since the threshold τ_{th} will essentially depend on the breaker trip-times in the grid, this value is not specified for Algorithm 2, and all the designed feedback matrices are considered to be time-feasible for the purpose of simulations. The closed-loop linearized system is then simulated (with the initial state x_0 obtained from nonlinear simulations) to obtain the predicted closed-loop response of the system, so as to select the ‘best’ $K^* \in \bar{K}$. These results are shown in Table II for the three designed controllers with varying levels of sparsity. It is seen that all controllers are stabilizing, and that as the level of sparsity increases, the closed-loop performance degrades along with an increase in execution time. We also see that the controller $K_{\mathcal{H}_2}$ from [6] provides much lower block-sparsity as compared all three of our designed controllers, with a comparable closed-loop performance. Keeping the trade-off for performance and sparsity in mind, we choose $K^* = K_2 \in \Omega_2$ as the best choice for this disturbance scenario.

Fig. 2 compares the Fast Fourier Transform (FFT) of the open-loop system and closed-loop system with block-sparse $K^* \in \Omega_2$. It is seen that FFT magnitudes of the dominant modes (highlighted) are reduced in closed-loop. Also, the frequencies for the closed-loop inter-area modes do not differ significantly from the open-loop model. Simulations are also conducted on the nonlinear model, with $K^* \in \Omega_2$. Fig. 3 shows the closed-loop responses of the nonlinear model (Figs. 3(b),(d)) for the generator rotor speeds and the electric power for indicated generators, compared with their open-loop responses (Figs. 3(a),(c)). We see that our sparse controller K^* improves the system performance despite the presence of the nonlinearity in the plant model. It can,

TABLE I: MP matrix showing residue magnitudes for the NE system with parallelization sets highlighted, with $\mu_1 = 0.76$, $\mu_2 = 1.79$ and $\mu_3 = 3.17$.

	λ_1 (0.12 Hz)	λ_2 (0.14 Hz)	λ_3 (0.32 Hz)	λ_4 (0.63 Hz)	λ_5 (0.92 Hz)	λ_6 (1.03 Hz)	λ_7 (1.07 Hz)	λ_8 (1.43 Hz)	λ_9 (1.53 Hz)
$\Delta\omega_1$	0.05	0.60	0.77	0.14	0.24	0.09	0.09	0.42	4.84
$\Delta\omega_2$	0.04	0.55	0.63	0.78	0.28	1.01	1.03	2.48	1.27
$\Delta\omega_3$	0.07	0.42	0.60	0.94	0.36	1.51	1.64	1.44	0.03
$\Delta\omega_4$	0.08	0.40	0.45	2.31	0.53	0.35	0.10	0.73	0.81
$\Delta\omega_5$	0.04	0.47	0.46	3.14	1.42	2.33	0.93	0.31	0.21
$\Delta\omega_6$	0.04	0.51	0.49	2.50	0.49	1.06	1.16	0.23	0.12
$\Delta\omega_7$	0.04	0.56	0.46	2.45	0.45	0.91	1.01	0.20	0.21
$\Delta\omega_8$	0.04	0.57	0.68	0.18	0.46	0.06	0.08	0.42	5.06
$\Delta\omega_9$	0.05	0.62	0.51	0.96	3.41	0.67	0.18	0.11	0.64
$\Delta\omega_{10}$	0.05	0.66	1.01	0.75	0.13	0.07	0.06	0.04	0.20

TABLE II: Simulation results using the three designed controllers, and the offline controller from [6].

$K_i \in \Omega_i$	block sparsity θ_i	exec. time τ_i (secs)	sub-opt. ind. ξ_i
K_1	32.7%	0.42	1.05%
K_2	72.7%	1.33	7.37%
K_3	92.7%	2.68	9.74%
$K_{\mathcal{H}_2}$	18.2%	15.15	8.03%

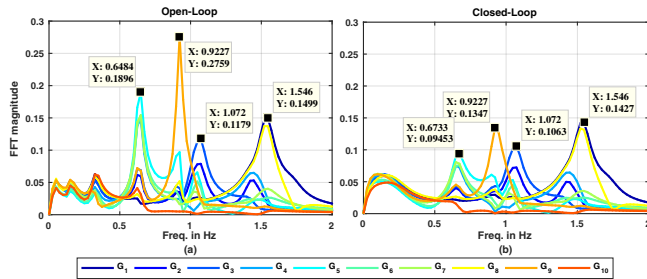


Fig. 2: (a) Open-loop and (b) closed-loop frequency response for all rotor speed outputs of all NE system generators.

therefore, be considered as robust to linearization. It also saves on the number of communication links as compared to a centralized controller.

VI. CONCLUSIONS

This paper develops an online algorithm for suppressing inter-area oscillations in power systems using sparse communication. The structure of the communication graph is decided from the physical characteristics of the power system model using online modal analysis. The control design is online in the sense that the ‘initial’ state of the system is estimated by a central control entity immediately after the occurrence of a disturbance. Stability for the constrained control problem is achieved via a generalized Riccati equation method. Simulation results on a 39-bus power system model show the effectiveness of our approach.

REFERENCES

[1] P. Kundur, *Power system stability and control*. McGraw-hill New York, 1994, vol. 7.

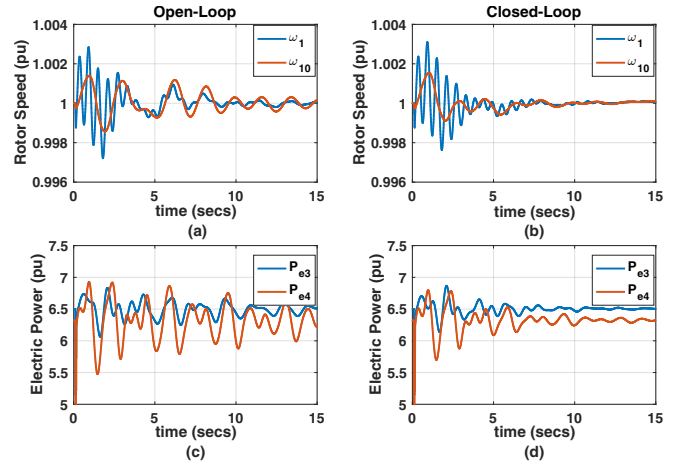


Fig. 3: Nonlinear simulations for open- and closed-loop with $K^* \in \Omega_2$. Subfigs (a)-(b) compare the rotor speeds for Gens. 1, 10, and (c)-(d) compare the electric power for Gens. 3, 4.

[2] B. Chaudhuri and B. C. Pal, “Robust damping of multiple swing modes employing global stabilizing signals with a TCSC,” *Power Systems, IEEE Transactions on*, vol. 19, no. 1, pp. 499–506, 2004.

[3] A. C. Zolotas, B. Chaudhuri, I. M. Jaimoukha, and P. Korba, “A study on LQG/LTR control for damping inter-area oscillations in power systems,” *Control Systems Technology, IEEE Transactions on*, vol. 15, no. 1, pp. 151–160, 2007.

[4] A. Jain, E. Biyik, and A. Chakraborty, “A model predictive control design for selective modal damping in power systems,” in *American Control Conference (ACC)*, July 2015, pp. 4314–4319.

[5] A. Chakraborty and P. P. Khargonekar, “Introduction to wide-area control of power systems,” in *American Control Conference (ACC)*, 2013. IEEE, 2013, pp. 6758–6770.

[6] F. Dorfler, M. R. Jovanovic, M. Chertkov, and F. Bullo, “Sparsity-promoting optimal wide-area control of power networks,” *Power Systems, IEEE Transactions on*, vol. 29, no. 5, pp. 2281–2291, 2014.

[7] A. Heniche and I. Kamwa, “Control loops selection to damp inter-area oscillations of electrical networks,” *Power Systems, IEEE Transactions on*, vol. 17, no. 2, pp. 378–384, 2002.

[8] F. Lian, A. Duel-Hallen, and A. Chakraborty, “Ensuring economic fairness in wide-area control for power systems via game theory,” in *American Control Conference (ACC)*, 2016, pp. 3231–3236.

[9] E. V. Larsen, J. J. Sanchez-Gasca, and J. H. Chow, “Concepts for design of FACTS controllers to damp power swings,” *Power Systems, IEEE Transactions on*, vol. 10, no. 2, pp. 948–956, 1995.

[10] J. Geromel, A. Yamakami, and V. Armentano, “Structural constrained controllers for discrete-time linear systems,” *Journal of optimization theory and applications*, vol. 61, no. 1, pp. 73–94, 1989.